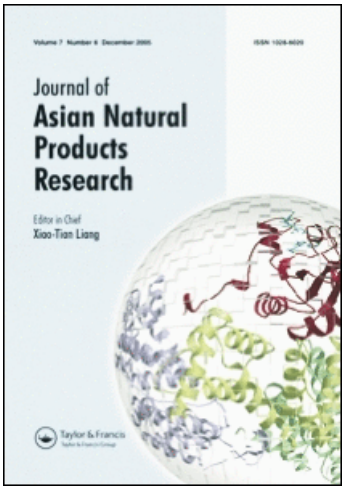

Journal of Asian Natural Products Research
Publication details, including instructions for authors and subscription information:
http://www.informaworld.com/smpp/title~content=t713454007

Effects of osthole on apoptosis and TGF-β_1 of hypertrophic scar fibroblasts

Xiao-Hua Hou[a]; Bo Cao[b]; Hong-Qi Liu[a]; Yi-Zheng Wang[bc]; Shu-Fang Bai[b]; Hong Chen[bc]
[a] Affiliated Hospital of Medical College of Chinese People's Armed Police Forces, Tianjin, China [b] Department of Pharmacognosy, Medical College of Chinese People's Armed Police Forces, Tianjin, China [c] Tianjin Key Laboratory for Biomarkers of Occupational and Environmental Hazard, Tianjin, China

To cite this Article Hou, Xiao-Hua , Cao, Bo , Liu, Hong-Qi , Wang, Yi-Zheng , Bai, Shu-Fang and Chen, Hong(2009) 'Effects of osthole on apoptosis and TGF-β_1 of hypertrophic scar fibroblasts', Journal of Asian Natural Products Research, 11: 7, 663 — 669
To link to this Article: DOI: 10.1080/10286020902975772
URL: http://dx.doi.org/10.1080/10286020902975772

Journal of Asian Natural Products Research
Vol. 11, No. 7, July 2009, 663–669

Taylor & Francis
Taylor & Francis Group

Effects of osthole on apoptosis and TGF-β_1 of hypertrophic scar fibroblasts

Xiao-Hua Hou[a], Bo Cao[b], Hong-Qi Liu[a], Yi-Zheng Wang[b,c], Shu-Fang Bai[b] and Hong Chen[b,c]*

[a]*Affiliated Hospital of Medical College of Chinese People's Armed Police Forces, Tianjin 300162, China;* [b]*Department of Pharmacognosy, Medical College of Chinese People's Armed Police Forces, Tianjin 300162, China;* [c]*Tianjin Key Laboratory for Biomarkers of Occupational and Environmental Hazard, Tianjin 300162, China*

(*Received 23 February 2009; final version received 15 April 2009*)

Osthole, 7-methoxy-8-[3-methylpent-2-enyl]coumarin (**1**), was extracted from a Chinese herb *Cnidium monnieri* (L.) Cuss. It showed immunity strengthening, anti-tumor, anti-hepatitis, and anti-osteoporosis activities in previous studies. Our goals are to study the effects of **1** on cell proliferation and TGF-β of hypertrophic scar fibroblasts. Our results showed that **1** induced apoptosis and inhibited cell proliferation in hypertrophic scar fibroblasts. 3-(4,5-Dimethylthiazol-2-yl)-2,5-diphenyltetrazolium bromide (MTT) assay showed that its IC_{50} value toward hypertrophic scar fibroblasts was 15.5 ± 2.2 μmol/l. Furthermore, the results of cell growth curve matched with the above results. Inducing apoptosis by **1** in hypertrophic scar fibroblasts was assessed by various morphological and biochemical characteristics, including cell shrinkage, chromatin condensation, membrane blebbing, formation of apoptotic bodies, and DNA ladder formation. A typical 'Sub-G_1 peak' was also checked through flow cytometry. We used immunohistochemistry to observe the expression of TGF-β_1. Also, we found that **1** could obviously inhibit the expression of TGF-β_1 of fibroblasts derived from hypertrophic scar compared with the control group ($P < 0.05$). These results suggest that **1** inhibits the growth of hypertrophic scar fibroblasts through apoptosis and decreases the expression of TGF-β_1.

Keywords: osthole; hypertrophic scar; apoptosis; TGF-β_1

1. Introduction

Hypertrophic scar is a unique human dermal fibroproliferative disorder that occurs after trauma, inflammation, burns, surgery, and possibly spontaneously. Although it is not fatal, it can significantly affect the patient's quality of life. The mechanism of hypertrophic scar is still unclear and there is no effective therapy for it. In the last decade, more attention has been given to uncover the benefits of the natural products in relation to hypertrophic scar. Osthole (Figure 1), a natural coumarin compound (**1**), was isolated from a Chinese herb *Cnidium monnieri* (L.) Cuss [1]. It has been used for the treatment of pain in female genitalia, impotence, and suppurative dermatitis in ancient China [2]. It also showed antifertility effect [3,4] and was established as a general cytotoxic agent against P-388 lymphocytic leukemia, KB carcinoma of the nasopharynx,

*Corresponding author. Email: chenhongtian06@yahoo.com.cn

ISSN 1028-6020 print/ISSN 1477-2213 online

DOI: 10.1080/10286020902975772
http://www.informaworld.com

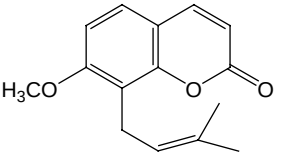

Figure 1. Chemical structure of **1**.

HT-1080 fibrosarcoma, human breast cancer, human melanoma, human lung cancer, and human colon cancer cells [5,6] *in vitro*. Failure of apoptosis has been postulated to cause the hypercellularity and thus the excess scar-tissue formation of hypertrophic scars [7]. A dysregulation in Fas-mediated apoptosis that normally occurs during the process of wound healing may be an important mechanism by which keloids arise and that TGF-β_1 is an important factor responsible for this resistance [8].

For the first time, our results showed that **1** inhibits the growth of hypertrophic scar fibroblasts through apoptosis and downregulates the expression of TGF-β_1.

2. Results and discussion

2.1 Effect of 1 on the growth of hypertrophic scar fibroblasts

The growth of fibroblasts was inhibited by **1** at different concentrations (5–50 μmol/l). The inhibition efficiency of fibroblasts increased up to 84.81% when treated with 32 μmol/l of **1**. The IC_{50} value was 15.5 ± 2.2 μmol/l.

Furthermore, the results of cell growth curve of fibroblasts matched with the above results (Figure 2).

2.2 Osthole inducing apoptosis

Osthole induced morphological changes, which were characteristics of apoptosis in fibroblasts (Figures 3 and 4). Contrast cells displayed excellent growth characteristics. Osthole evoked typical apoptotic features such as membrane blebbing, cell shrinkage and detachment, and nuclear condensation and fragmentation.

Flow cytometric analysis of fibroblasts exposed to **1** confirmed the above morphological observations. The DNA fluorescence histograms of Hoechst-stained cells showed that low DNA stainability of the osthole-treated apoptotic cells resulted in a distinct and quantifiable region below the G_1 peak. By contrast, the G_1 peak predominated in control cells (Figure 5). Quantification of dose dependency was done by monitoring the amount of nuclei with subdiploid DNA content using flow cytometry (Figure 6). The percentage of apoptotic cells increased

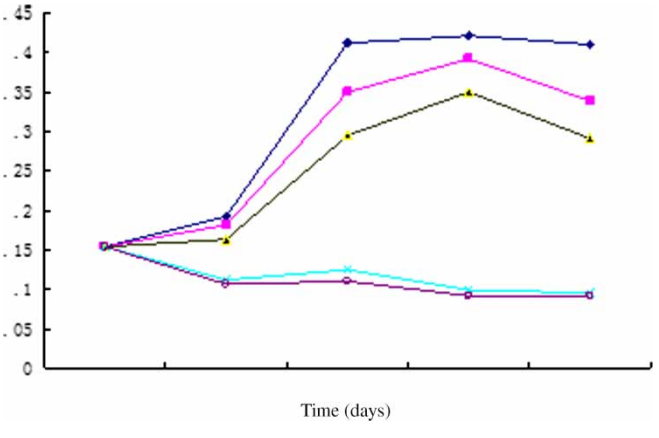

Figure 2. Effect of **1** on the growth of fibroblasts, and fibroblasts treated with **1** (10–45 μmol/l).

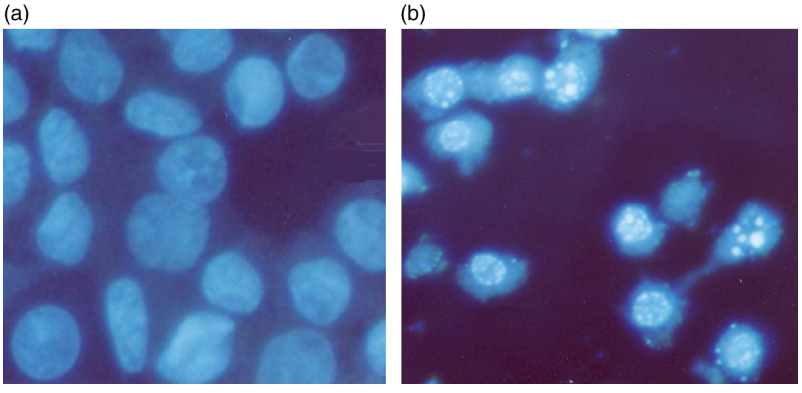

Figure 3. Morphological appearance of cells by fluorescence detection. (a) Fibroblasts treated with 0.1% DMSO; (b) fibroblasts treated with 32 μmol/l of **1**. P (× 400).

when the concentration of **1** increased, and a dose dependency was observed.

Finally, agarose gel electrophoresis showed a typical DNA fragmentation pattern of apoptosis (Figure 4). DNA fragmentation caused by **1** was also dose-dependent; the intensity of DNA fragmentation increased when the amounts of **1** (10–32 μmol/l) were increased.

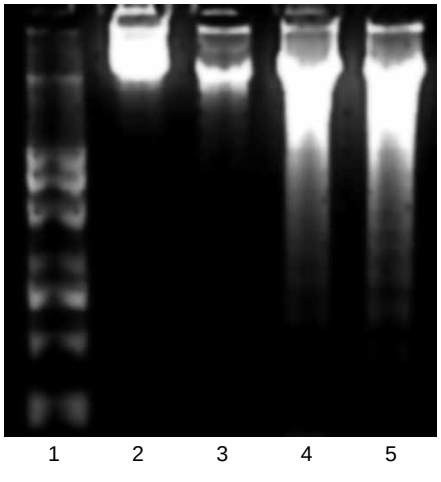

Figure 4. Osthole-induced DNA fragmentation in fibroblasts. DNA was separated and analyzed on agarose gel as described in Section 3. Lane 1, DNA size marker, fibroblasts untreated (lane 2), and treated with 5, 10, and 20 μmol/l (lanes 3–5) of **1** for 24 h. Demonstration of apoptosis by gel electrophoresis. DNA extracted from fibroblasts untreated or exposed to increasing concentrations of **1** (10–32 μmol/l) for 24 h was separated by agarose gel (1.5%) and stained with ethidium bromide.

2.3 Effect of 1 on the expression of TGF-β_1 of hypertrophic scar fibroblasts

Immunocytochemistry was applied to detect the expression of TGF-β_1 in hypertrophic scar fibroblasts. There was a significant difference in the TGF-β_1 expression between the control group and the experimental group with the positive percentages (21.5 ± 2.7)%, (19.9 ± 2.2)%, and (14.0 ± 1.8)%, respectively ($P < 0.05$; Figure 7).

Hypertrophic scar formation is a wound healing response, which fails to resolve and leads to the formation of a raised collagen mass extending beyond the original wound margins. The pathophysiology of this process remains unknown. Each year, millions of trauma and burn injuries give rise to hypertrophic scars resulting in disfigurement and dysfunction [9,10]. Apoptosis is a form of physiological cell death, characterized by chromatin condensation, cytoplasmatic blebbing, and DNA fragmentation [11]. A dysregulated apoptotic process is involved in the excessive accumulation of the extracellular matrix [12,13]. Fibroblasts are the main effector cells in wound healing process, and can proliferate,

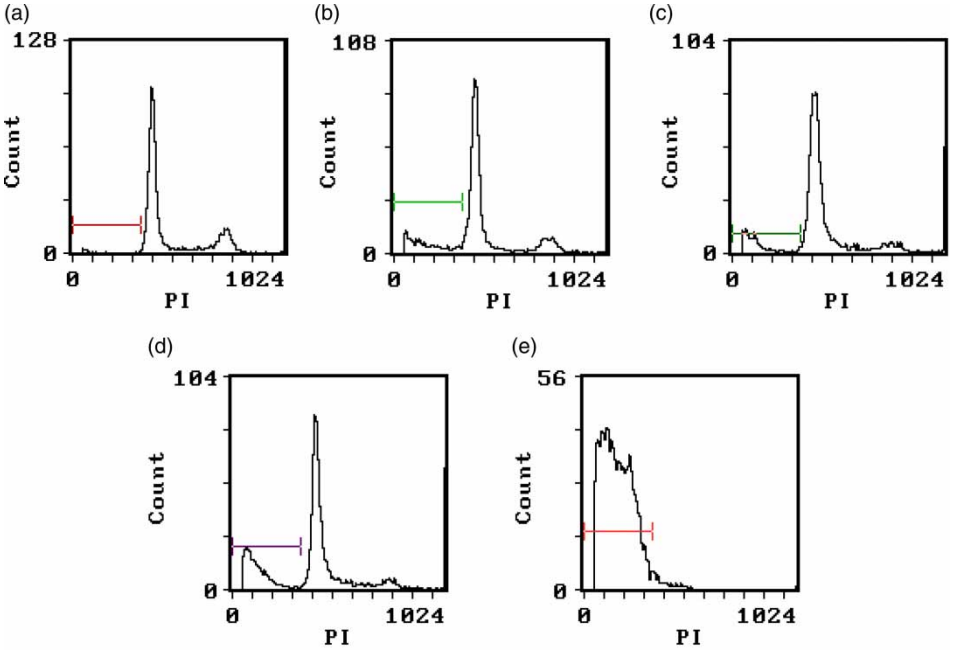

Figure 5. Demonstration of apoptosis by flow cytometric analysis. (a) Untreated fibroblasts. (b)–(e) Appearance of cells with subdiploid DNA content after exposure to increasing concentrations of **1** (10, 16, 32, and 50 μmol/l) for 24 h.

migrate, secrete to the extracellular matrix, and differentiate into myofibroblasts. Messadi *et al.* [14] used an Annexin-V-FITC binding assay to show that normal skin fibroblast cultures were found to have a twofold higher percentage of apoptotic cells than hypertrophic scar fibroblast culture. More evidence

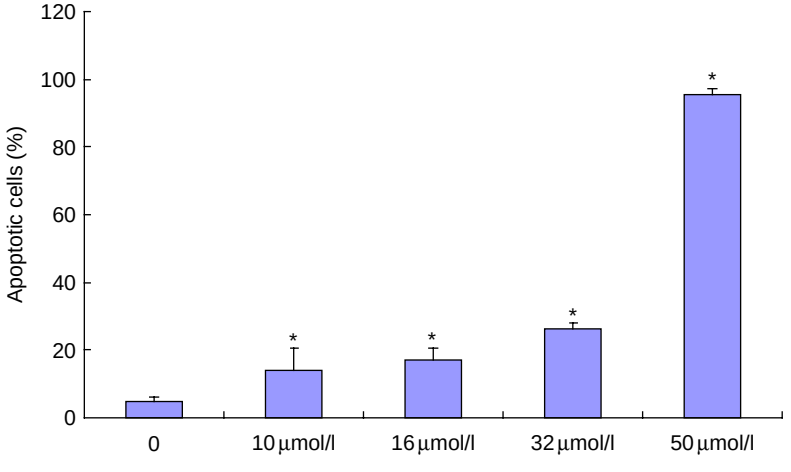

Figure 6. Dose-dependent induction of apoptosis by **1**. Cells were incubated with increasing concentrations of **1** for 24 h. Percentage of apoptotic cells and percentage of cells with subdiploid DNA content as described in Section 3.

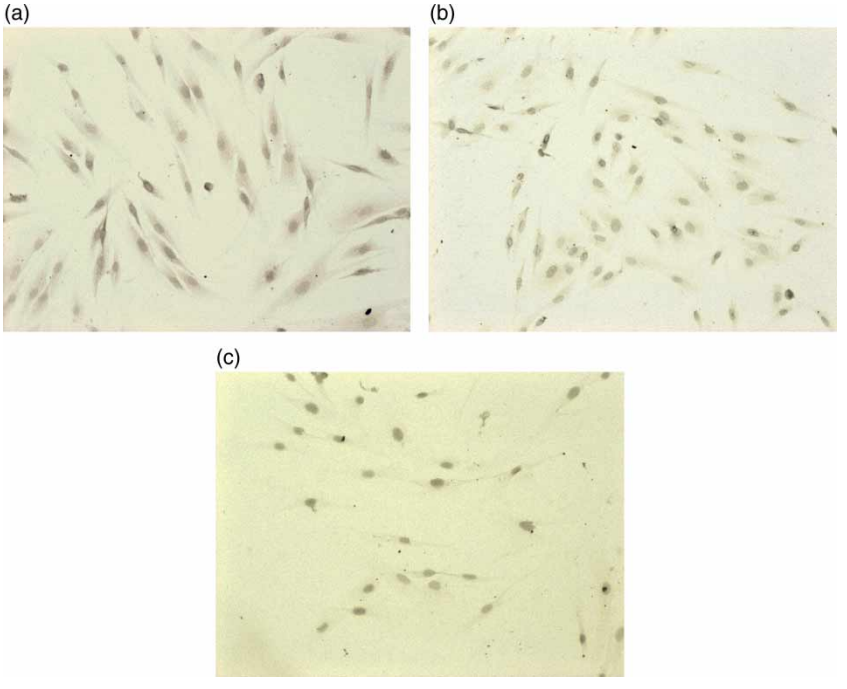

Figure 7. Effect of **1** on TGF-β_1 expression in fibroblasts. Fibroblasts were continuously exposed to **1** (10–32 μmol/l); TGF-β_1 expression determined by immunohistochemistry as described in Section 3. (a) 0.1% DMSO; (b) and (c) 10–32 μmol/l osthole.

showed that the development of a hypertrophic scar might be related to the decrement of apoptotic fibroblasts [15,16]. Our results showed that **1** can induce fibroblast apoptosis, and dose dependency was observed.

TGF-β is a potent factor thought to be involved in keloid pathogenesis [17,18]. More and more evidence showed that the downregulation of TGF-β_1 can inhibit scar hyperplasia. TGF-β is important in almost every step in the process of tissue fibrosis by simultaneously signaling fibroblasts to increase the synthesis of matrix proteins, decrease the production of matrix-degrading proteases, and increase the production of inhibitors of these proteases [19]. Our results showed that **1** can decrease the expression of TGF-β_1 in hypertrophic scar fibroblasts.

In summary, our results first showed that **1** inhibited hypertrophic scar through induced apoptosis of fibroblasts and downregulated the expression of TGF-β_1.

3. Experimental

3.1 General experimental procedures

Osthole (**1**), purchased from NICPBP (Beijing, China), and its purity was >98%. It was dissolved in dimethylsulfoxide and further diluted in cell culture medium before use. The final concentration of DMSO in the solution was <0.1%. It was stored at 4°C before use. Proteinase K, RNase A, SDS Na, acrylamide, and Hoechst 33342 were purchased from Sigma Chemical Co. (St Louis, MO, USA). Dulbecco's modified Eagle's medium (DMEM), trypsin, propidium iodide, Tris, and MES were products of Gibco Laboratories (Grand Island, NY, USA). Mouse monoclonal anti-TGF-β_1 and horseradish peroxidase-conjugated anti-mouse IgG were purchased from Beijing

Zhongshan Golden Bridge Biotechnology Co. Ltd (Beijing, China).

3.2 Cell culture

Fibroblast cultures were initiated from mature human burn scar tissue following surgical excision for reconstruction. The epidermis and any remaining fat were excised from the scar tissue with the aid of magnifying loupes. The 0.5 cm^2 pieces of tissue were placed in culture flasks, and using an explant technique, burn scar fibroblasts were cultured. Growth medium consisted of DMEM, L-glutamine, streptomycin/penicillin (all Gibco), and fetal bovine serum. The growth medium was changed every second day. Fibroblasts were grown in the moist atmosphere of a CO_2 incubator (5% CO_2, 95% air) at 37°C. The cells were grown to confluence and then to a maximum passage for further experimentation. Six patients were included in this study. Their age ranged from 15 to 50, and they included three women. The age of scar proliferation ranged from 3 to 6 months. Tissue culture was adopted and the second-generation cell was applied for the test.

3.3 MTT assay

The cells were detached by trypsinization, seeded at 2.0×10^3 cells/well in a 96-well microtiter plate overnight, and treated with different concentrations of **1** in DMEM with 10% fetal bovine serum. The effects on cell growth were examined by the MTT assay. Finally, 50 μl of the MTT solution (1 mg/ml in DMEM) was added to each well and incubated at 37°C for 4 h. The MTT–formazan formed by metabolically viable cells was dissolved in 150 μl of DMSO, and monitored by a microplate reader at dual wavelengths of 570 and 450 nm, and the IC_{50} values were defined as the drug concentrations that inhibited the cell number to 50% after 96 h. The experiment was repeated at least thrice and the combined data were compared by Student's paired *t*-test.

3.4 Cellular growth curve control

The cells in the log phase were trypsinized and seeded at 2.0×10^3 cells/well in a 96-well microtiter plate. The effects on the cell growth were examined by the MTT assay every 24 h for five successive days in order to compose the growth curve *in vitro*.

3.5 Assessment of apoptosis by Hoechst

To analyze chromatin condensation, which is a sign of apoptosis, 1×10^4 cells were added to each well of the 24-well plates. The cells were exposed to **1** (32 μmol/l) for 24 h, and Hoechst staining was performed. The final concentration of Hoechst 33342 is 5–10 μg/ml. At first, 4% formaldehyde solution was added to each well in which cells had been exposed to **1**. The cells were then incubated with the dilute Hoechst 33342 for 10 min at room temperature. Finally, each well was examined under a fluorescence microscope equipped with a DM455 filter for chromatin condensation.

3.6 Assessment of apoptosis by flow cytometry

Trypsinized cells were washed with phosphate-buffered saline (PBS) and then fixed with 70% ethanol. The fixed cells were kept at least overnight at −20°C. The cells were washed with PBS before analysis, and then the fluorochrome solution (50 μg/ml propidium iodide in PBS, plus RNase, 50 μg/ml) was added. The distribution of the cell cycle phases was determined by analytical flow cytometry using a Coulter Epics XL (Coultronics France SA, Margency, France), with an excitation/emission of 488/525 nm. All experiments were performed thrice.

3.7 Assessment of apoptosis by DNA fragmentation

The cells incubated with **1** (10–32 μmol/l) for 24 h were collected and washed twice by PBS, then resuspended in 0.5 ml of the extraction buffer (100 mmol/l NaCl, 10 mmol/l Tris–HCl, pH 8.0, 25 mmol/l EDTA, pH 8.0, 0.1 mg/ml proteinase K) at 50°C for 12 h. DNA was extracted with an equal volume of saturated phenol–chloroform–isoamyl alcohol (25:24:1) and extracted again with a combination of chloroform–isoamyl alcohol (24:1), then centrifuged at 12,000*g* for 30 min. The precipitated DNA was analyzed on a 1.5% agarose gel.

3.8 TGF-β_1 immunohistochemistry

Cells were plated into a Lab-TeK Chamber Slide at a density of 2×10^4 cells/well and grown until approximately 80% confluent, after which they were treated with **1** at 10–32 μmol/l for 24 h, as described previously. The cells were washed, fixed in ice-cold methanol for 10 min, and then soaked in PBS containing 2% Triton X-100 for 5 min to increase their permeability to antibodies. These cells were exposed to anti-TGF-β_1 antibodies (1:100) at 4°C overnight. After washing, bound primary antibodies were incubated in the appropriate secondary antibody, and then visualized by 3,3′-diaminobenzidine tetrahydrochloride. Images were collected using the microscope and Image-Pro Plus (Media Cybernetics, Wokingham, Berkshire, UK).

References

[1] E. Li, A.M. Clark, and C.D.J. Hufford, *J. Nat. Prod.* **58**, 57 (1995).
[2] S.P. Yang, Y. Wang, Y. Wu, and J.M. Yue, *J. Nat. Prod.* **65**, 1041 (2002).
[3] Y.L. Zhang, R.Z. Lu, and A.L. Yan, *Acta Pharmacol. Sin.* **11**, 60 (1990).
[4] S.P. Yang, L. Dong, Y. Wang, Y. Wu, and J.M. Yue, *Bioorg. Med. Chem.* **11**, 4577 (2003).
[5] D.J. Pan, Z.L. Li, C.Q. Hu, K. Chen, J.J. Chang, and K.H. Lee, *Planta Med.* **56**, 383 (1990).
[6] B.N. Zhou, *Mem. Inst. Oswaldo Cruz* **86**, 219 (1991).
[7] C. Linge, J. Richardson, and C. Vigor, *J. Invest. Dermatol.* **125**, 72 (2005).
[8] T. Chodon, T. Sugihara, H.H. Igawa, E. Funayama, and H. Furukawa, *Am. J. Pathol.* **157**, 1661 (2000).
[9] P. Martin, *Science* **276**, 75 (1997).
[10] A.J. Singer and R.A. Clark, *N. Engl. J. Med.* **341**, 738 (1999).
[11] D.T. Loo and J.R. Rillema, *Methods Cell Biol.* **57**, 251 (1998).
[12] R.C. Williams, Jr. and J.C. Lee, *Methods Enzymol.* **85**, 376 (1982).
[13] S. Aarabi, K.A. Bhatt, Y. Shi, and J. Paterno, *FASEB J.* **21**, 3250 (2007).
[14] D.V. Messadi, A. Le, S. Berg, and A. Jewett, *Wound Repair Regen.* **7**, 511 (1999).
[15] A. Nakazono-Kusaba, F. Takahashi-Yanaga, Y. Miwa, and S. Morimoto, *Eur. J. Pharmacol.* **497**, 155 (2004).
[16] T. Chodon, T. Sugihara, H.H. Igawa, E. Funayama, and H. Furukawa, *Am. J. Pathol.* **157**, 1661 (2000).
[17] G.S. Chin, W. Liu, Z. Peled, and T.Y. Lee, *Plast. Reconstr. Surg.* **108**, 423 (2001).
[18] I.J. Lim, T.T. Phan, C. Song, W.T. Tan, and M.T. Longaker, *Plast. Reconstr. Surg.* **107**, 797 (2001).
[19] W.A. Border and N.A. Noble, *N. Engl. J. Med.* **331**, 1286 (1994).